

Transient Study of an Automata-Based Microgrid Supervisory Control

Zhi Jin (Justin) Zhang, Arman Ghasaei, Reza Iravani

Abstract—This paper investigates and demonstrates transient performance of a microgrid supervisory control (SC) subjected to extreme conditions, e.g., light load condition, and highlights its feature to provide transition between viable discrete operational scenarios. In contrast to the conventional automata-based SCs, the envisioned SC is designed and synthesized based on Supervisory Control Theory. The studies show that PI-based local controllers of the microgrid’s distributed resource units can follow the SC switch-mode commands and maintain the microgrid operational. The reported studies are conducted in a hybrid MATLAB/PSCAD platform where the SC is represented in MATLAB and the power circuitry is modeled in PSCAD.

Keywords—Discrete-event systems, microgrid transients, supervisory control.

I. INTRODUCTION

MICROGRIDS are regarded as a key enabler of high-depth penetration of distributed energy resources (DERs). A microgrid supervisory controller (SC) is required to i) determine operational mode of the microgrid subsequent to a pre-determined or an accident event, ii) coordinate operation of various generation and energy storage units, and iii) dispatch appropriate generation units depending on the operating condition, i.e., load and generation profiles, for realization of a microgrid. Finite-state machines (FSMs)/finite-state automata have been widely adopted for implementing SCs due to the discrete behavior of supervision.

FSM-based SCs for microgrids have been reported in [1]–[3]. However, their SCs are not synthesized in a systematic fashion; hence, there is no guarantee that the proposed synthesis procedures can be replicated for other microgrids. Supervisory Control Theory (SCT) [4] provides a systematic procedure for SC design. In SCT, the design process amounts to creating meaningful plant models and control specifications; then synthesizing the supervisory controller follows as an automated computational task.

Reference [5] has demonstrated the applicability of SCT to an AC microgrid, which consists of a battery energy storage system (BESS), a photovoltaic (PV) unit, and a synchronous generator, by systematically designing an automata-based decentralized SC for the islanded operation of the microgrid. This work serves as a continuation of [5] by i) investigating an adverse operating scenario, i.e., extreme light load, that leads to system collapse and proposing a solution based on switching

the grid-forming unit using SCT, ii) examining the transients that arise when multiple DER units are switching their discrete modes of operation simultaneously, as commanded by the SC, by implementing detailed models of the DERs, and iii) studying the effects of communication delays between the SC and local controllers (LCs) on microgrid transients. This work also investigates if conventional PI-based LCs [6] are able to seamlessly transition from one operation state to another, especially during the switching of the grid-forming unit in the microgrid. Although SCT-based solution to only the light load condition is proposed, the heavy load solution can be generated *mutatis mutandis* owing to the systematic nature of the supervisor synthesis procedure.

The remainder of this paper is organized as follows. Section II introduces the study system, and Section III shows the supervisory control that is derived from SCT to satisfy operational requirements of the microgrid. Section IV presents the simulation results to show the transient performance during the extreme light load condition and the impact of non-identical communication delays. Section V concludes the paper.

II. STUDY SYSTEM

The microgrid under study, as shown in Fig. 1, is composed of i) 27.6-kV, three-phase, overhead, distribution-class lines, ii) a 3-MW, 3-MWh, 1.2-kV BESS, iii) one 2-MW solar PV unit, iv) a 6-MW synchronous generator (GEN) unit, and v) a total of 4.3-MVA balanced loads with 0.93 to 0.99 lagging power factors (PF). A battery management system (BMS) and a phase-locked loop (PLL) monitor and report the battery’s state-of-charge and the system frequency at PCC in Fig. 1 to the SC, respectively.

III. ORIGINAL OPERATIONAL STRATEGY

Only islanded mode of operation is discussed; in this mode, the system voltage is solely controlled by the BESS to stay within the permitted range [7] and the SC dynamically dispatches appropriate resources, i.e., BESS, GEN, and PV unit, to keep the microgrid frequency within its prescribed limit [7]. The original operational strategy from [5] is summarized in Table I.

A. Supervisory Control Synthesis

This section provides a summary of the synthesis procedure of the decentralized supervision structure, based on SCT, that fulfills the above-mentioned operational strategy for the microgrid in Fig. 1 as discussed in [5]. In this work, we assume

Z. J. Zhang, A. Ghasaei, and R. Iravani are with the University of Toronto, Toronto, ON M5S 3G4, Canada (e-mail of corresponding author: justin.zhang@mail.utoronto.ca).

Paper submitted to the International Conference on Power Systems Transients (IPST2019) in Perpignan, France June 17-20, 2019.

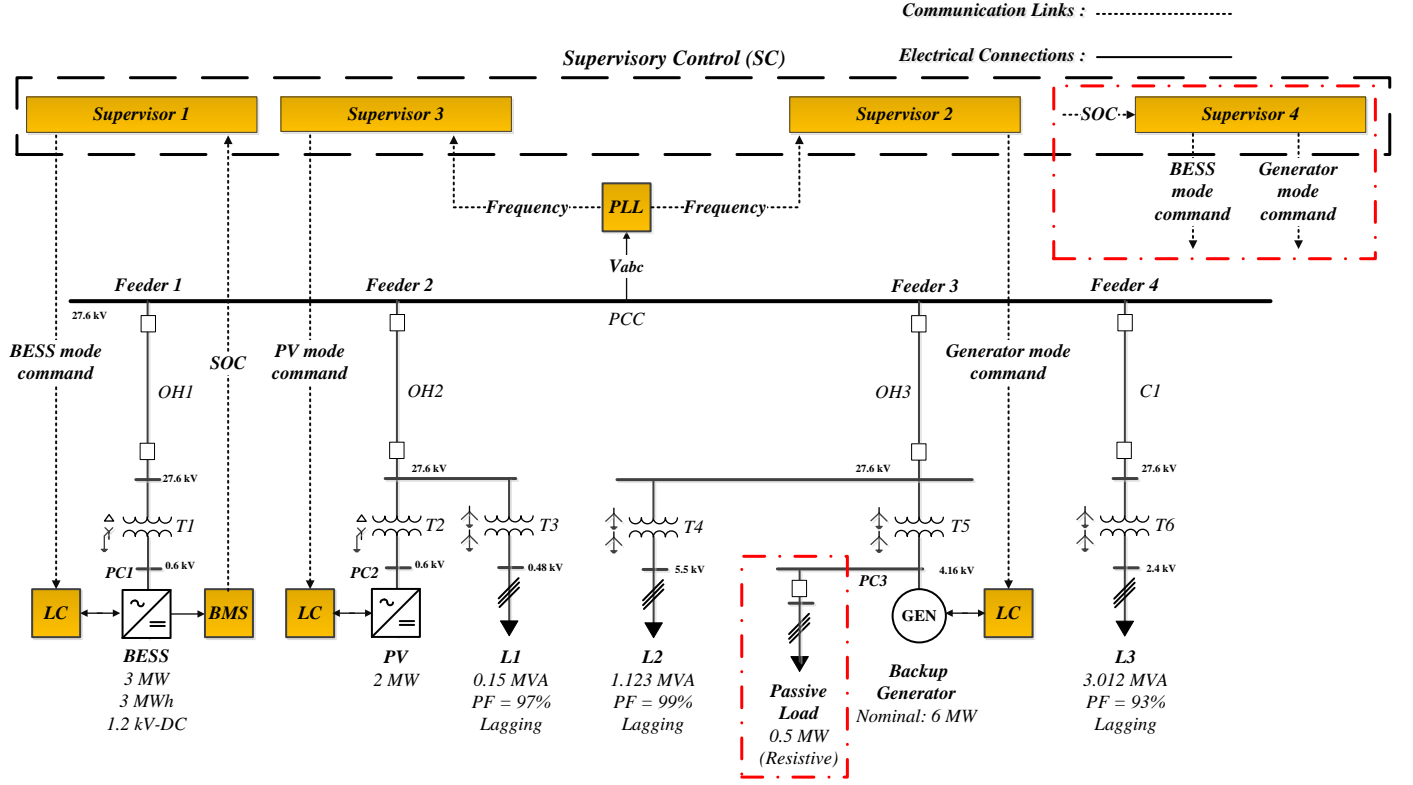


Fig. 1. Single-line diagram of the study system and the two-level hierarchical control structure (note that Supervisor 4 and Passive Load in red dotted-dashed boxes are only present in the proposed supervisory control solution in Section IV-B).

TABLE I
DISTRIBUTED RESOURCE UNITS OPERATIONAL STRATEGY

DER Unit	State	Operational Strategy
BESS	0: $30\% < SOC < 80\%*$	Normal mode: The BESS controls the system frequency in an open-loop manner through its internal oscillator, whose frequency is dynamically varied from $59.964 Hz^{\ddagger}$ to $60.036 Hz^{\ddagger}$ corresponding to $SOC = 30\%$ to $SOC = 80\%$.
	1: $SOC \leq 30\%^{\dagger}$ or $SOC \geq 80\%^{\dagger}$	Critical mode: The BESS controls the system frequency in a closed-loop manner based on a $P-f$ droop strategy (P is input and f is output) in conjunction with either the PV unit or GEN [8].
PV	0: $f < 60.036 Hz$	The PV unit operates in the maximum power point tracking (MPPT) mode at unity power factor.
	1: $f \geq 60.036 Hz$	The PV unit enters curtailment mode, i.e., its active power output is curtailed based on a $f-P$ droop structure (f is input and P is output) at unity power factor.
GEN	0: $f > 59.964 Hz$	The GEN stays in the standby mode, i.e., injecting a constant output active power of 0.05 MW (0.83% of nominal power) in the microgrid.
	1: $f \leq 59.964 Hz$	The GEN enters rated condition, i.e., initially increasing output power to its rated value of 5.58 MW (93% of nominal power) to charge the BESS and then its power is re-adjusted based on a $f-P$ droop structure.

* SOC limits should be application-specific, i.e., defined based on the type of battery used. In this paper, the lower and upper limits are set at 30% and 80% respectively merely to demonstrate that the supervisory control is functional.

\ddagger The frequency range is defined such that an adequate margin is maintained from the allowable critical limits of $59.500 Hz$ and $60.500 Hz$ based on [7].

\dagger A 2% hysteresis band is applied to the SOC limits in the actual implementation to prevent multiple transitions, e.g., the SC switches BESS to critical mode when SOC reaches 82% and 28% and commands BESS to normal mode when SOC returns to 78% and 32%, respectively.

i) all events in the microgrid are observable, ii) the supervisory control acts based on one contingency at a time, and iii) the measured signals, e.g., frequency and SOC, are 100% accurate (no specific types of measurement sensors are considered).

The plant components, i.e., BESS, PV unit, GEN, BMS, and PLL are modeled using automata in the software platform *TCT*, which is a computer program for synthesizing supervisory controls for discrete-event systems (detailed information on *TCT* can be found in [4]). The BESS, PV unit, and GEN are modeled as two-state automata, shown in Figs. 2(a), 2(b), and 2(c), respectively. The automata states correspond to those listed in Table I. For example, state 0 of the GEN indicates that it is in the standby mode. In *TCT*,

controllable/uncontrollable events are designated by odd/even numbers, respectively. For instance, events 21 and 23 are the transitions between MPPT and curtailment modes of the PV unit, which are controllable, meaning the SC is able to enable/disable these events.

The BMS of the BESS, depicted in Fig. 2(d), has four distinct events where events 72 and 76 signal that the SOC has reached its lower and upper limits, respectively, and event 74 indicates that the SOC is within its prescribed range. Event 71 is the initialization event for the BMS. The models of BESS and BMS are independent from each other and are only linked via the operational strategy presented in Table I. The PLL, shown in Fig. 2(e), is a

three-state automata with five different events. Events 62 and 66 indicate that the system frequency has reached its upper and lower limits, respectively, and event 64 identifies that the frequency is within its prescribed range. Events 61 and 65 are the initialization events for over-frequency and under-frequency signal measurements, respectively. Note that the even-numbered events are uncontrollable, i.e., they cannot be disabled by SC, because both the SOC and frequency levels depend on the system operating condition, i.e., load and generation.

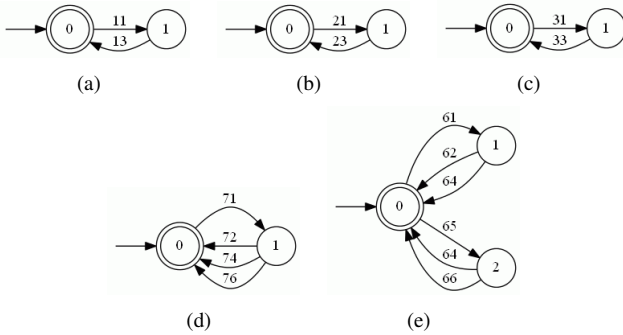


Fig. 2. Models of: (a) battery energy storage system, (b) photovoltaic system, (c) backup generator, (d) battery management system, and (e) phase-locked loop.

Based on SCT, three decentralized supervisors are generated. Each supervisor controls one part of the plant: Supervisor 1 (Fig. 3(a)), Supervisor 2 (Fig. 3(b)), and Supervisor 3 (Fig. 3(c)) control the BESS, GEN, and PV unit, respectively.

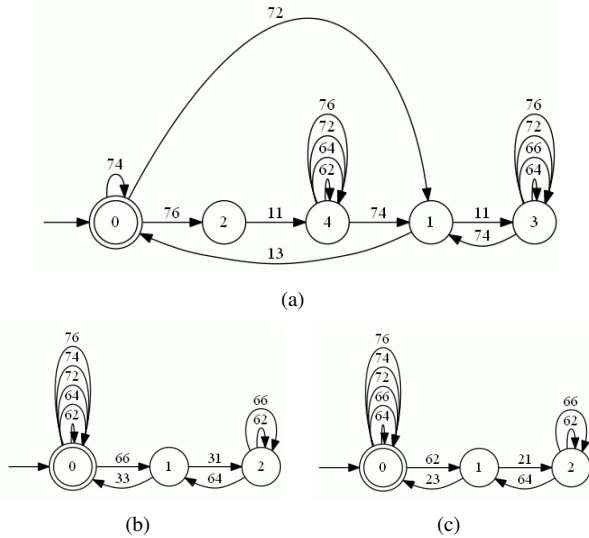


Fig. 3. Decentralized supervisors: (a) Supervisor 1, (b) Supervisor 2, and (c) Supervisor 3.

IV. TRANSIENT PERFORMANCE EVALUATION

The microgrid power circuit, local controllers, PLL and BMS are modeled in the PSCAD time-domain simulation software package, whereas the decentralized supervisors of Figs. 3(a) to 3(c), which interface with the microgrid local

controllers, are implemented in the MATLAB Stateflow toolbox. In order to study system transients, detailed voltage-sourced converter models [6] for the battery storage system and PV unit and a 6th-order synchronous machine model of the synchronous generator are implemented in the simulations. All model parameters are chosen based on industry-grade inverters and generators with similar ratings. Furthermore, a communication delay of 25 ms between each decentralized supervisor and its corresponding local controller [9] is considered to represent the average communication latency in microgrids of the similar size to the one in Fig. 1.

A. Extreme Light Load Condition

Fig. 4(a) depicts the the BESS transition from normal to critical state and the PV unit from MPPT to curtailment mode at approximately 48.8 seconds. Note that the actual transition command occurs at $SOC = 82\%$ due to the aforementioned hysteresis mechanism implemented in the SC. The frequency and voltage dynamics are shown in Figs. 4(b) and 4(c), respectively, which are within the prescribed range of NERC standard [7].

A load decrease of 1 MW was imposed at 50 seconds in order to enter the extreme light load condition, and the SOC can be observed to increase as a result. The BESS disconnects when its SOC has reached either the maximum or minimum allowable limit [10], and in this paper, the maximum SOC limit is set to 98%. The SOC increased to this limit at approximately 57.9 seconds, and the BESS disconnected from the microgrid for self-protection. Subsequently, no further control action was taken. Hence, as the only grid-forming device was off-line, the frequency is observed to continue increasing and the microgrid became susceptible to external disturbances. A sudden load step increase of 1 MW occurred at 63 seconds, and the microgrid has collapsed as a result.

Although this study case demonstrates the local controllers are able to maintain the system operational when the PV unit output power is curtailed, neither the SC nor LCs can prevent system collapse in case of a further load reduction. One solution is to trip the PV unit in order to start discharging the BESS; nevertheless, it is desired to keep all DERs operational for as long as possible. Therefore, the approach proposed in this work is based on re-designing the supervisory control without tripping the PV unit.

B. Proposed Supervisory Control Solution

As mentioned previously, the supervisory control has to take preemptive actions before the SOC reaches its maximum limit. Thus, the new operational strategy specifies that if the SOC has reached 90% [8], then the BESS must transition to grid-following mode where only discharge is allowed and the GEN has to start to form the grid. In this scenario, the system voltage and frequency are maintained through the generator's excitation system and the droop structure between the PV unit and GEN, respectively, since the PV unit is still in the curtailment mode. The BESS output power set-point varies from 0.09 MW to 1 MW corresponding to $SOC = 90\%$ to $SOC = 95\%$. We formalize this strategy by i) modify the

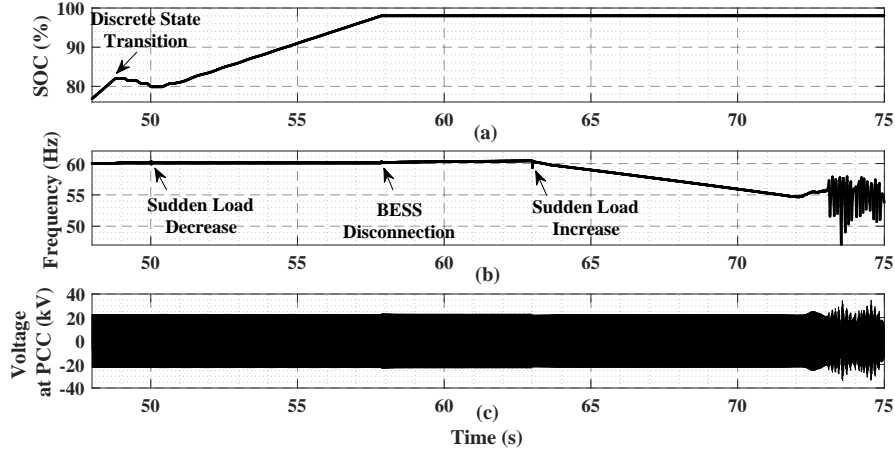


Fig. 4. Impact of light load condition on microgrid: (a) SOC, (b) system frequency, and (c) PCC voltage.

individual plant component models, and ii) synthesize a new set of supervisors.

The BESS model, shown in Fig. 5(a), is changed to include a new state, i.e., state 2, that corresponds to the grid-following mode when its $SOC \geq 90\%$, and events 41 and 43 are transitions between the grid-forming and critical ($SOC \leq 30\%$ or $80\% \leq SOC < 90\%$) modes of operation. The new GEN model (Fig. 5(b)) has a new state that indicates its grid-forming operation. The BMS model, depicted in Fig. 5(c), has two new events: event 70 signals the SOC has reached 90% and event 75 is the initialization event that will be discarded during controller synthesis. Other two plant component models, i.e., PV unit and PLL, do not need to be modified; this modular approach shows the generality and simplicity features of SCT.

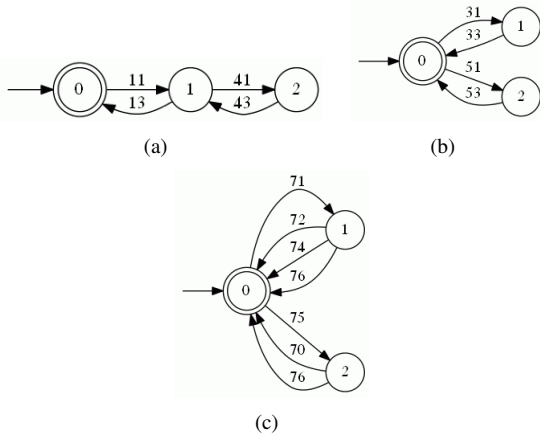


Fig. 5. New models of: (a) BESS, (b) GEN, (c) BMS.

The overall microgrid DES model, obtained by combining the component DES models, has 162 states and 1296 transitions, which makes manual design and verification of supervisory control an extremely difficult task. Nonetheless, from the systematic synthesis process provided by SCT, a new supervisory controller was generated that includes the ones in Fig. 3 and an additional supervisor of Fig. 6 (Supervisor

4) [4], [5]. Then it was systematically verified that the four supervisors do not conflict with each other and their collective action is nonblocking.

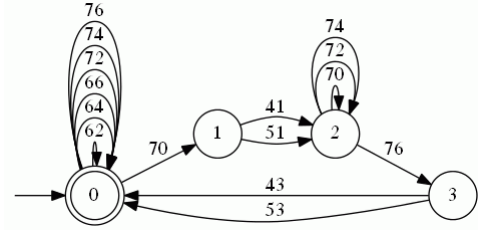


Fig. 6. Additional supervisor Supervisor 4.

Due to the necessity of communication between Supervisor 4 and both the BESS and GEN, the supervision structure is no longer decentralized and is considered to be distributed [11]. In addition, the proposed approach only requires another grid-forming device to be available, which may be an inverter-based resource, and does not necessarily rely on having a synchronous generator in the microgrid.

C. Extreme Light Load Condition Revisited

Since the new operational strategy involves switching the grid-forming unit (changing the slack bus), this discrete-event transition may induce severe dynamics, which needs to be examined in order to validate the proposed supervisory control. Aside from implementing anti-windup mechanisms, the following measures are taken to make the mode transition smooth:

- The BESS discharge set-point is set to a small value (0.09 MW) when it enters or exits the grid-following mode;
- A ramp limiter is added so that the BESS output power varies slowly when switching between grid-forming and grid-following modes;
- A ramp limiter in the governor of the generator is implemented to slowly change its output power when switching between standby and grid-forming modes. It is a normal practice for a rotating machine to ramp up/down its output power at a particular rate.

Furthermore, a passive load, e.g., a braking resistor, of 0.5 MW is connected to $PC3$ in Fig. 1 to act as a minimum load in the system and absorb any extra power whenever the generator is forming the grid, because, generally it is not practical for a synchronous generator to change into motoring mode [12].

Figs. 7(a) to 7(c) show the SOC level, and the frequency and voltage dynamics, respectively, when the SOC reached 92% around 55.84 seconds and the BESS/GEN transitioned into grid-following/grid-forming mode at approximately 55.86 seconds owing to the communication delay. The system frequency briefly dropped to 58.7 Hz, but recovered in 40 ms; the PCC voltage momentarily dropped to 0.91 p.u. before increasing to 1.05 p.u. Both the frequency and voltage are within the NERC limits. After this transition, the GEN output power, depicted in Fig. 7(d), can be observed to ramp up from 0.05 MW to around 0.5 MW, and the BESS output power, depicted in Fig. 7(e), eventually would change from charging (negative value) to discharging (positive value), which happened gradually as imposed by the ramp limiter.

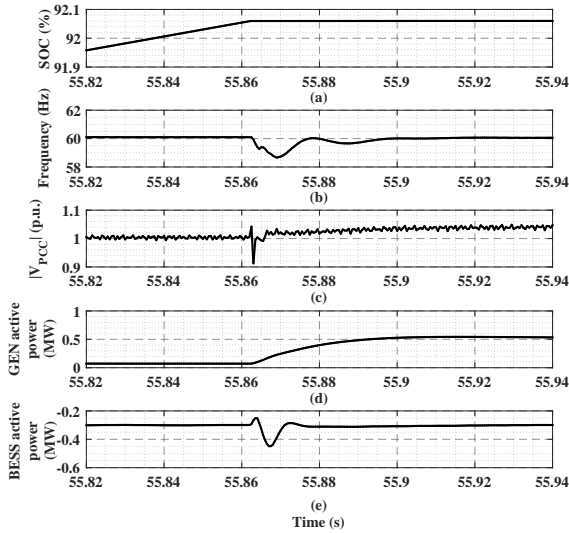


Fig. 7. Microgrid dynamics when the GEN became the grid-forming unit: (a) SOC, (b) system frequency, (c) PCC voltage, (d) GEN output active power, and (e) BESS output active power.

Figs. 8(a) to 8(c) depict the SOC level, and the frequency and voltage dynamics, respectively, when, at 60 seconds, a load of 0.7 MW was imposed on the microgrid, which caused an acceptable undershoot in the frequency. The GEN output power (Fig. 8(d)) increased correspondingly to 1.27 MW, until this load was removed 2 seconds later. The load removal caused an acceptable overshoot in the frequency. During this period, the BESS output power (Fig. 8(e)) did not change since it was not contributing in forming the grid, and the PCC voltage, dictated by the generator exciter, was well stabilized.

Figs. 9(a) to 9(c) present the SOC level, and the frequency and voltage dynamics, respectively, when, at approximately 66.69 seconds, the SOC dropped to 88% and the GEN and BESS returned back to standby and critical states, respectively, around 66.72 seconds. The frequency increased to 64.7 Hz, and recovered within 100 ms; voltage dropped to 0.97 p.u. and its fluctuations settled down in 95 ms. Even though the

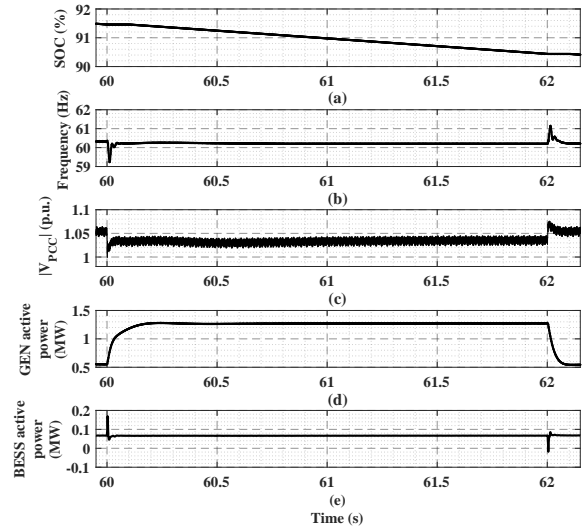


Fig. 8. Microgrid dynamics due to a load step change: (a) SOC, (b) system frequency, (c) PCC voltage, (d) GEN output active power, and (e) BESS output active power.

transients are more severe than those of the transition in Fig. 7, they are still within the permitted range by NERC. The severity can be explained by noting that in these two transitions, the generator and battery system start to form the grid, respectively; however, the generator has inertia, thereby limiting both the frequency and voltage excursions as compared to the BESS. The GEN output active power (Fig. 9(d)) would eventually drop to 0.05 MW; this happened gradually as imposed by the ramp limiter.

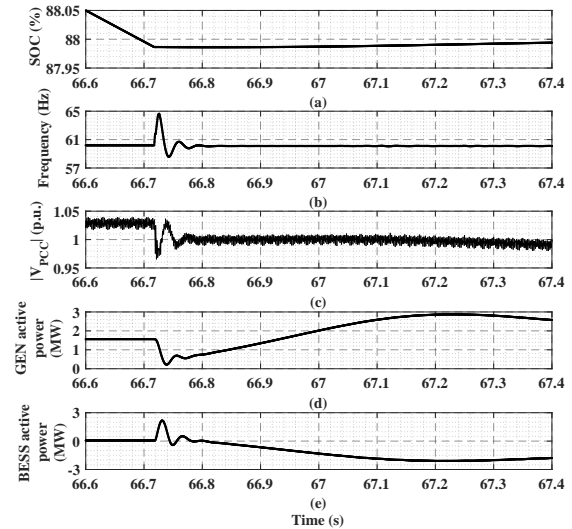


Fig. 9. Microgrid dynamics when the GEN switched back to standby mode: (a) SOC, (b) system frequency, (c) PCC voltage, (d) GEN output active power, and (e) BESS output active power.

Throughout the generator grid-forming period, the PV unit stayed in the curtailment mode because the SOC was always greater than 80%. Compared to the results in Section IV-A, the new supervisory control was able to maintain the microgrid operational in the extreme light load condition; because a

grid-forming device always existed, a sudden load change did not lead to system collapse. This validates the solution presented in Section IV-B.

D. Impact of Communication Delay

The communication delay in previous study cases is assumed to be 25 ms , but the delays between the SC and each DER unit's LC are not necessarily equal [9]. This non-identical delay may be problematic for the switching of the grid-forming unit as commanded by Supervisor 4, because if the GEN command reaches its local controller faster than that of the BESS, then when the SC makes the BESS the grid-forming device, for the duration of this non-identical delay, there will be no device to form the grid. On the contrary, there can be two grid-forming devices when the SC commands the BESS to enter grid-forming mode with a delay. Therefore, we need to find the maximum non-identical delay between the BESS and GEN during grid-forming transitions that will keep the microgrid operational. We assume that system conditions are unchanged during the non-identical delay.

By increasing the non-identical delay until the system dynamics reached the NERC limits in simulation, it was observed that the maximum non-identical delay between the BESS/GEN command and its LC can only be 100 ms longer than that between the GEN/BESS command and its LC. One of the worst-case scenarios occurs when the SC commands the BESS and GEN to switch back to grid-forming and standby modes, respectively, as depicted in Fig. 10. The BESS command, presented in Fig. 10(a), reached its LC at 65.97 seconds. The GEN command, shown in Fig. 10(b), was received by the LC at 66.07 seconds. The frequency (Fig. 10(c)) first increased to 65.9 Hz and then decreased to 58.1 Hz ; the PCC voltage (Fig. 10(d)) decreased to 0.93 p.u. and then reached 1.07 p.u. Both frequency and voltage recovered within 130 ms . Their dynamic responses are within the prescribed NERC limits.

If the BESS/GEN command reaches its LC more than 100 ms later than that of the GEN/BESS, the frequency dynamics will become unacceptable. Note that 100 ms is only an estimation obtained from simulation and may change for different systems. However, the results show that it is desired to design communication links such that the delays in the BESS and GEN commands are similar.

V. CONCLUSIONS

This paper is a continuation of [5] by investigating state transition transients in an AC microgrid. System dynamics in the extreme light load condition is simulated, and a new supervisory control is synthesized via a systematic procedure to extend the previous operational limit. Also, the maximum delay between the SC and the BESS and GEN LCs is examined. The simulation results show that:

- The proposed SC is able to prevent the microgrid from collapse in the extreme light load condition;
- PI-based local controllers are capable of transition from one operation state to another, including switching of the grid-forming device, with acceptable frequency and voltage dynamics;

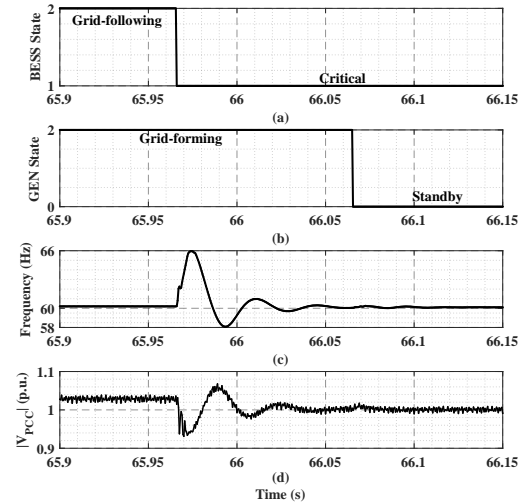


Fig. 10. Impact of communication delay for switching the grid-forming unit: (a) BESS state, (b) GEN state, (c) system frequency, and (d) PCC voltage.

- The delays in communication for the BESS and GEN commands should be made as close as possible.

Future work should focus on applying this methodology to large-scale systems and examine the impact of measurement errors on the proposed approach.

REFERENCES

- [1] J. Wang, C. Zhao, A. Pratt, and M. Baggu, "Design of an advanced energy management system for microgrid control using a state machine," *Applied Energy*, vol. 228, pp. 2407–2421, 2018.
- [2] Y. Karimi, H. Oraee, M. S. Golsorkhi, and J. M. Guerrero, "Decentralized method for load sharing and power management in a pv/battery hybrid source islanded microgrid," *IEEE Transactions on Power Electronics*, vol. 32, no. 5, pp. 3525–3535, 2017.
- [3] M. Saleh, Y. Esa, and A. Mohamed, "Centralized control for dc microgrid using finite state machine," in *Power & Energy Society Innovative Smart Grid Technologies Conference (ISGT), 2017 IEEE*. IEEE, 2017, pp. 1–5.
- [4] W. M. Wonham and K. Cai, *Supervisory Control of Discrete-Event Systems*. Springer-Verlag, 2018.
- [5] A. Ghasaei, Z. J. Zhang, R. Iravani, and W. M. Wonham, "Systematic design of a microgrid discrete power management strategy," Submitted to *IEEE Transactions on Control Systems Technology*, 2018.
- [6] A. Yazdani and R. Iravani, *Voltage-Sourced Converters in Power Systems: Modeling, Control, and Applications*. John Wiley & Sons, 2010.
- [7] *Performance of Distributed Energy Resources During and After System Disturbance*, North American Electric Reliability Corporation, 2013.
- [8] N. L. Díaz, A. C. Luna, J. C. Vasquez, and J. M. Guerrero, "Centralized control architecture for coordination of distributed renewable generation and energy storage in islanded ac microgrids," *IEEE Transactions on Power Electronics*, vol. 32, no. 7, pp. 5202–5213, 2017.
- [9] P. Kansal and A. Bose, "Bandwidth and latency requirements for smart transmission grid applications," *IEEE Transactions on Smart Grid*, vol. 3, no. 3, pp. 1344–1352, 2012.
- [10] M. Zeraati, M. E. H. Golshan, and J. M. Guerrero, "Distributed control of battery energy storage systems for voltage regulation in distribution networks with high pv penetration," *IEEE Transactions on Smart Grid*, vol. 9, no. 4, pp. 3582–3593, 2018.
- [11] D. E. Olivares, A. Mehrizi-Sani, A. H. Etemadi, C. Canizares, R. Iravani, M. Kazerani, A. H. Hajimiragha, O. Gomis-Bellmunt, M. Saeedifard, R. Palma-Behnke *et al.*, "Trends in microgrid control," *Smart Grid, IEEE Transactions on*, vol. 5, no. 4, pp. 1905–1919, 2014.
- [12] M. Goyal and R. Gupta, "Operation and control of a distributed microgrid with hybrid system," in *Power Electronics (IICPE), 2012 IEEE 5th India International Conference on*. IEEE, 2012, pp. 1–6.